ISSN 0915-633X

INTERNATIONAL ATOMIC ENERGY AGENCY

SIXTEENTH IAEA FUSION ENERGY CONFERENCE

Montréal, Canada, 7-11 October 1996

IAEA-CN-64/CP-3

NATIONAL INSTITUTE FOR FUSION SCIENCE

A Study on Density Profile and Density Limit of NBI Plasmas in CHS

S. Morita, H. Idei, H. Iguchi, S. Kubo, K. Matsuoka, T. Minami, S. Okamura, T. Ozaki, K. Tanaka, K. Toi, R. Akiyama, A. Ejiri, A. Fujisawa, M. Fujiwara, M. Goto, K. Ida, N. Inoue, A. Komori, R. Kumazawa, S. Masuzaki, T. Morisaki, S. Muto, K. Narihara, K. Nishimura, I. Nomura, S. Ohdachi, M. Osakabe, A. Sagara, Y. Shirai, H. Suzuki, C. Takahashi, K. Tsumori, T. Watari, H. Yamada and I. Yamada

(Received - Aug. 26, 1996)

NIFS-440 Sep. 1996

RESEARCH REPORT
NIFS Series

NAGOYA, JAPAN

INTERNATIONAL ATOMIC ENERGY AGENCY

SIXTEENTH IAEA FUSION ENERGY CONFERENCE

Montréal, Canada, 7-11 October 1996

IAEA-CN-64/ CP-3

A Study on Density Profile and Density Limit of NBI Plasmas in CHS

S.Morita, H.Idei, H.Iguchi, S.Kubo, K.Matsuoka, T.Minami, S.Okamura, T.Ozaki, K.Tanaka, K.Toi, R.Akiyama, A.Ejiri, A.Fujisawa, M.Fujiwara, M.Goto, K.Ida, N.Inoue, A.Komori, R.Kumazawa, S.Masuzaki, T.Morisaki, S.Muto, K.Narihara, K.Nishimura, I.Nomura, S.Ohdachi, M.Osakabe, A.Sagara, Y.Shirai, H.Suzuki, C.Takahashi, K.Tsumori, T.Watari, H.Yamada and I.Yamada

National Institute for Fusion Science, Nagoya 464-01, Japan

Keywords: Hydrogen neutral particle, Neutral energy, Density profile, Density limit, Plasma collapse

A Study on Density Profile and Density Limit of NBI Plasmas in CHS

Abstract

The mechanism of density profile formation has been studied in CHS. It has been generally known that the profiles become peaked and hollow in limiter- and divertor-dominated cases, respectively. This tendency does not change for the direction of NBI such as co- and counter-injection resulting a difference of the electric field. It is also found that the density profiles are not affected by the magnetic configuration itself. The density profile, however, is influenced by the limiter insertion. Edge ion temperatures were correlated with density peaking factor of $n_{e0}/\langle n_e \rangle$. As a result, it was found that a peaked profile ($n_{e0}/\langle n_e \rangle \geq 1.5$) can be obtained with higher edge ion temperature ($\geq$40ev at ρ=0.9). These results indicate the importance of energy distribution of incoming neutral particles. An analysis is done to explain the results. On the other hand, the density limit has been also studied in CHS NBI plasmas. It was found that the density limit was strongly affected by the density profile. Some discussions are made on the mechanism related to the density limit.

1. Introduction

In helical plasmas the density profiles have a large variation in comparison with tokamak in which the hollow and flat density profiles can not be easily produced. In tokamak the inward particle velocity is frequently introduced to describe the peaked density profile, although in helical devices it is believed that the velocity is very small. The ExB force between the toroidal electric field and the poloidal magnetic field in tokamak is too weak to explain the inward velocity. The physical understanding is insufficient at present to explain the density profiles and the mechanism for the density profile formation is still an open question.

In CHS, at least, the density profiles are seemed to change according to a variety of the experimental conditions like R_{ax}, magnetic configurations, n_e and P_{heat} etc. Furthermore, the density limit and the density profile frequently change according to the wall conditioning method like Ti-gettering and boronization which present a different condition between wall recycling and gas puffing rates. Experiments have been carried out to study the mechanism of the density profile and the density limit formation. In this paper results are described on a study of density profile and density limit obtained from NBI plasmas ($n_e \leq 1 \times 10^{14} cm^{-3}$, $T_e \leq 2$keV, $T_i \leq 0.6$keV) of Compact Helical System (CHS heliotron/torsatron: $\langle a \rangle /R = 0.2/1.0$m, $B_t \leq 2$T, $l/m = 2/8$, $P_{NBI} = 1.1+0.7$MW, $P_{ECH} = 0.2+0.5$MW).

2. Magnetic Configuration of CHS

In CHS the LCFS is defined by the inner wall of the vacuum vessel for $R_{ax} \leq 94.9$cm since the major radius of the center of the vacuum vessel is 100cm, and it is called "limiter-dominated configuration". On the contrary, for $R_{ax} \geq 97.4$cm a small clearance begins to appear between the inner wall and the

LCFS, which is called "divertor-dominated configuration". The clearance becomes 1cm for R_{ax}=99.5cm and 4cm for R_{ax}=101.6cm. The magnetic well is performed for almost all configurations, at least in the core region, except for the case of R_{ax}=88.8cm. The helical ripple ε_h is less than 2% at the axis position for $R_{ax} \leq 94.9$cm and it increases when the R_{ax} is shifted outward (ε_h=8% for R_{ax}=101.6cm).

3. Density Profiles of NBI Plasmas

Figure 1 shows a typical example of the density profiles obtained from NBI plasmas (B_t=0.9T) [1]. There is a clear tendency that the peaked density profile is performed in the limiter-dominated configuration and the flat or hollow density profile is performed in the divertor-dominated configuration. In the case of limiter-dominated configuration the actual limiter area at the inner wall occupies 7-8% of the total plasma surface. The hydrogen particle influx from the inner wall limiter Γ_{lim} to the total influx Γ_{tot} is approximately 40% at $\langle n_e \rangle = 4 \times 10^{13} cm^{-3}$ for the R_{ax}=89.9cm case. For the R_{ax}=101.6cm case the Γ_{lim} disappears and the gas puffing rate is increased instead of it. The particle influx rate Γ_{gp}/Γ_{tot} from a location where the gas puffing is carried out reaches 20% for the R_{ax}=101.6cm case, whereas it is less than 10% for the R_{ax}=89.9cm case.

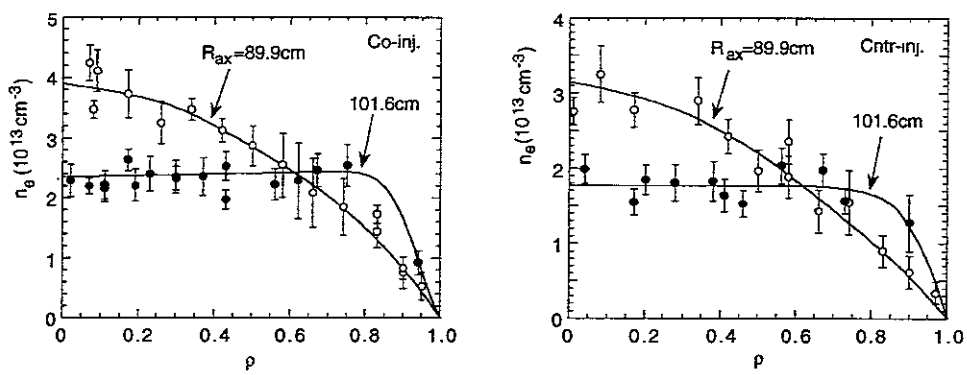

Fig.1 Radial profiles of n_e as a function of averaged radius ρ for two different magnetic axis cases. (left: co-inj., right: counter-inj.)

The comparison is also made between co- (Fig.1; left) and counter-NB (Fig.1; right) injection cases. It is very clear that there is no difference between the two. For the counter-injection case the large amount of the NB fast ions are lost by the inward shift of the drift orbit due to the ∇B drift under existence of the inner wall as a limiter. As a result it enhances an electric field and poloidal rotation. The rotation velocity reaches 10km/s at the plasma edge for the counter-injection case in the limiter-dominated configuration (R_{ax}=92.1cm) case, whereas it is less than 3km/s for the co-injection case. This result indicates that the electric field does not have any influence on the formation of the density profile.

The experiment was done by changing the NBI power for R_{ax}=92.1cm case to study an influence which the magnetic configuration directly gives on the density profile. In CHS the power dependence of the electron temperature is remarkable for the edge region rather than the central region. The result is shown in Fig.2. Two different profiles are obtained from the same configuration, although it is rare that such a hollow profile is obtained at R_{ax}=92.1cm. In the two discharges the edge T_e was very different as expected. Here, it should be noticed that the input power of the #2 NBI is decreased. For the hollow profile case it was 19eV at ρ=0.85 (T_{e0}=233eV), but for the peaked profile case it was 102eV (T_{e0}=353eV). The ion temperature also has the same tendency as the electron temperature. From this result it can be understood that the magnetic configuration does not directly give any effect on the density profile.

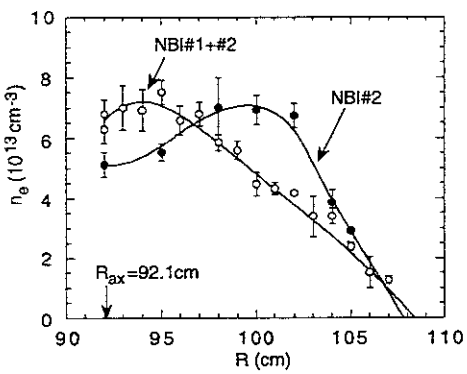

Fig.2 Two different radial n_e profiles obtained from the same configuration (R_{ax}=92.1cm). P_{NBI} is 0.9MW for #1 (counter-inj.) and 0.6MW for #2 (co-inj.).

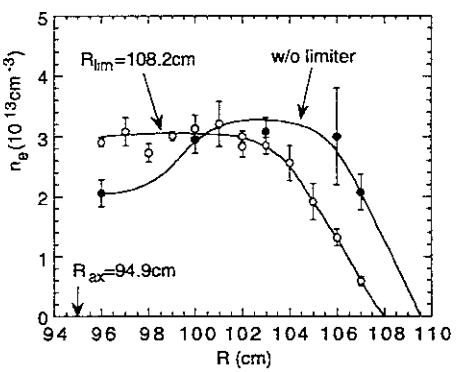

Fig.3 Radial n_e profiles before and after insertion of carbon-head limiter. The limiter was inserted (z=20mm) from the bottom of the vertically elongated position.

The limiter was inserted into NBI plasmas with a hollow density profile. The result is plotted in Fig.3. It is understood that the peaked density profile is realized after insertion of the limiter. The T_e profile does not change for the two cases. From this result we can understand that the density profile is strongly affected by the existence of the limiter.

The edge T_i (CVI charge exchange line) at ρ=0.9 is measured with the density peaking factor for different R_{ax} positions (see Fig.4), since the peak position of the radial neutral hydrogen distribution at the outside half along major radius side normally appears between ρ=0.90 and 0.95. The peaked density profiles tend to have a high edge T_i and are realized mainly for the limiter-dominated configuration. In contract to this, the flat density profiles have a low edge T_i for the divertor-dominated configuration. It is noticed that the recycling rate R becomes too large for the divertor-dominated cases. Especially for R_{ax}=101.6cm case, the value of R is close to 0.98 even in $n_e \leq 2 \times 10^{13}$cm^{-3} [2].

A similar relation between n_e profiles and edge T_i is obtained for the reheat-mode operation in the configuration of R_{ax}=94.9cm[3]. In the reheat-mode which is observed after switching off the gas puffing at high-density range, the density peaking can be also obtained with a large increase in the edge ion temperature. It is shown in Fig.5. Generally, in CHS, the density profiles become peaky for $R_{ax} \leq 92.1$ cases and become flat for $R_{ax} \geq 99.5$cm cases. For the cases of R_{ax}=94.9cm and 97.4cm, however, the density profiles are extremely sensitive to conditions of the vacuum wall surface. In other words the density profiles easily change according to each experimental week.

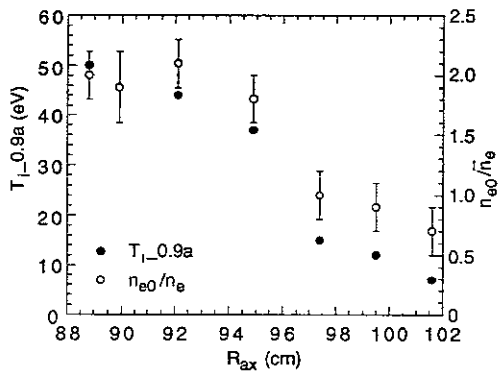

Fig.4 Comparison between edge T_i (ρ=0.9) and density peaking factor for different R_{ax} positions.

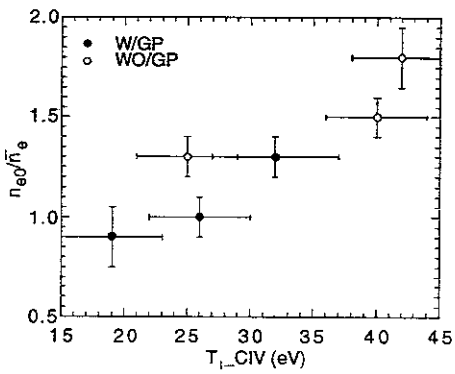

Fig.5 Density peaking factor as a function of edge Ti obtained from CIV(1548.2Å) broadening at R_{ax}=94.9cm case (solid circles: gas puffing case, open circles: reheat-mode case after gas puffing off).

The ionization length λ_i of neutral hydrogen is typically 4.7, 6.7 and 10.5cm for T_i=10, 20, 50eV cases at $n_e=3\times10^{13}$cm^{-3}, respectively. These values can easily change the neutral hydrogen profile and the density source term at core region. In the limiter-dominated configuration a direct distance (R_{ax}-R) between the inner wall surface (R=80cm) and the magnetic axis (R_{ax}) is very short. Therefore, the distance becomes equal to the λ_i when the energy of the neutrals increases. Detailed analysis is now being carried out. Typical example of the neutral hydrogen profile is shown in Fig.6. The Hα poloidal and toroidal locations are carefully measured in CHS[2]. The results are included in the calculation. The ion temperature measured from the Hα line profile gives a low value less than 1-2eV at the gas puffing position and a relatively high value of 7eV at the x-point. The particle fueling from the NBI is less than 20% for the total electron density at the plasma center. Therefore, the beam fueling has no large influence on the observed density profiles.

4. Relation between Density Limit and Density Profiles

Time behaviors of the electron densities at ρ=0.75 obtained from YAG Thomson system are plotted in Fig.7. The data are taken from 3 typical

discharges with and without plasma collapse. The line-averaged density was 4-5x10^{13}cm^{-3} at the end of the pulse for the 3 cases. It is understood that the edge density rise causes the plasma collapse at t=120ms. We can see the peaked density profiles are favorable for increasing the density limit. Figure 8 shows a comparison of the density profile ($n_e(0.75)/n_{e0}$) between collapsed and steady discharges. The results are similar to Fig.7.

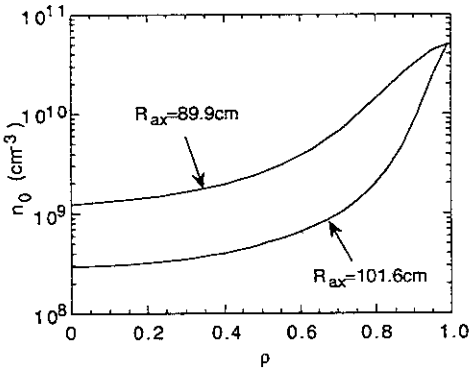

Fig.6 Calculation of neutral hydrogen profiles at cases of R_{ax}=89.9cm and 101.6cm. The profiles are normalized to the neutral density of 5x10^{10}cm^{-3} at ρ=1.0.

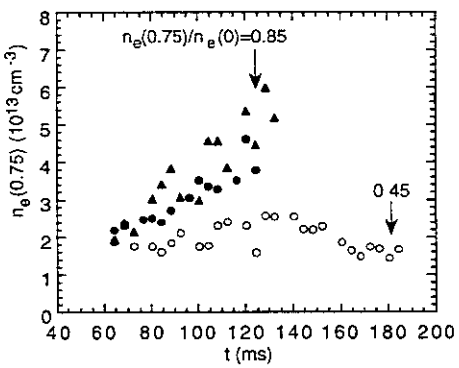

Fig.7 Time behavior of edge n_e ρ=0.75) from YAG Thomson measurement for typical 3 NBI discharges with (solid circles and triangles) and without (open circles) plasma collapse.

The obtained density limit is plotted against the peaking factor in Fig.9. These data are obtained with strongly carried out Ti gettering. The highest density achieved in CHS until now is 9x10^{13}cm^{-3} as a line-averaged density at B_t=1T. The further effort will be done at higher B_t range up to 2T and NBI power up to 2MW (1.1MW: #1, 0.7MW: #2). The higher values of the density limit shown in Fig.9 are obtained from the limiter-dominated configuration. In the counter-NBI case the density limit is lower than the co-injection case, since the fast ions in the counter-NBI case hit the inner-wall and the impurity buildup becomes serious. The density limit is extremely low for the co-injection case with the divertor-dominated plasmas. This combination lowers the net NBI power deposition. Moreover, in the Ti gettering case a large amount of the gas puffing is needed to get a density. This leads to the formation of the hollow density profiles and a further lowering of the NBI deposition power. Then, the low density limit for the divertor-dominated configuration can be improved for a high-recycling plasma like boronization[4,5]. In such a case the density limit reaches the same level as the limiter-dominated plasma, although the temperature is relatively low.

When the plasma collapses, the MHD instability is studied. At present, however, any correlation related to the collapse has not been obtained. Furthermore, the density limit for the R_{ax}=88.8cm configuration is comparable with other limiter-dominated configurations, whereas the m/n=2/1 sawtooth oscillation is excited because of the magnetic hill geometry. Then, these

observed values of the density limit are mainly restricted by the radiation and particle losses which are a strong function of the density profile.

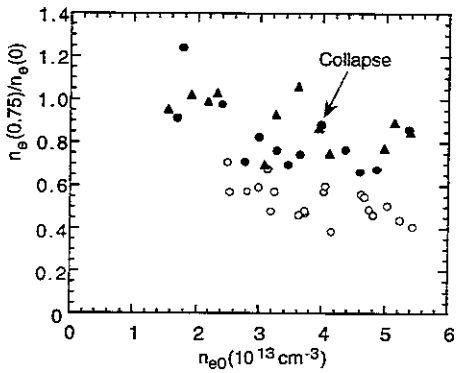

Fig.8 Density ratio of n_e at ρ=0.75 to n_e at ρ=0.0 as a function of n_e at ρ=0.0 (n_{e0}). Solid points indicate collapsed discharges (solid triangles: inner ρ=0.75, solid circles: outer ρ=0.75, open circles: both sides ρ=0.75).

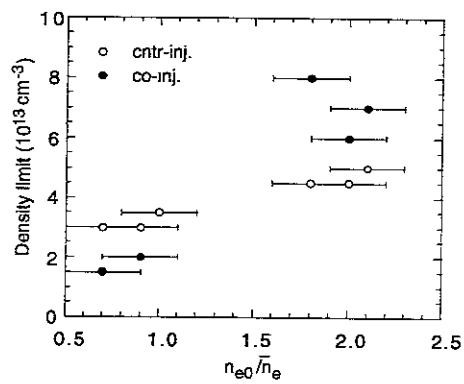

Fig.9 Density limit in CHS NBI plasmas as a function of density peaking factor obtained at B_t=1T and P_{NBI}=1MW under Ti-gettering (open circles: counter-injection case, solid circles: co-injection case).

5. Summary

The variations of the density profiles of NBI plasmas in CHS were observed by changing externally controlled plasma parameters like R_{ax}, direction of NBI, input power of NBI and limiter insertion. Through these studies it was found that the density profiles were strongly affected by the edge ion temperature. A possible candidate to explain the density profiles is a change in the neutral hydrogen profile as a source term. The density limit was also correlated with the density profiles. As a result, the peaked density profile is favorable for a rise of the density limit.

Acknowledgments

The authors thank all members of the torus group, especially Messrs. K.Motoki, S.Hattori and S.Ohtsuka, for their help in carrying out the experiments. The authors are also grateful to director-general Prof.A.Iiyoshi for his continuous encouragement.

References

[1] IGUCHI, H., et al., Plasma Phys. Cntrol. Fusion **36** (1994) 1091.
[2] MORITA, S., et al., Fusion Tech. **27** (1995) 239.
[3] MORITA, S., et al., in Plasma Physics and Controlled Nuclear Fusion Research 1992 (Proc. 14th Int. Conf. Würzburg, 1992), Vol.2, IAEA, Vienna (1993) 515.
[4] KANEKO, O., et al., in Plasma Physics and Controlled Nuclear Fusion Research 1990 (Proc. 13th Int. Conf. Washington, 1990), Vol.2, IAEA, Vienna (1991) 473.
[5] YAMADA, H., et al., Jpn.J.Appl.Phys. **33** (1994) L1638.

Recent Issues of NIFS Series

NIFS-399 K. Itoh, S-I. Itoh, A. Fukuyama and M. Yagi,
Theory of Self-Sustained Turbulence in Confined Plasmas; Feb. 1996

NIFS-400 J. Uramoto,
A Detection Method of Negative Pionlike Particles from a H2 Gas Descharge Plasma; Feb. 1996

NIFS-401 K.Ida, J.Xu, K.N.Sato, H.Sakakita and JIPP TII-U group,
Fast Charge Exchange Spectroscopy Using a Fabry-Perot Spectrometer in the JIPP TII-U Tokamak; Feb. 1996

NIFS-402 T. Amano,
Passive Shut-Down of ITER Plasma by Be Evaporation; Feb. 1996

NIFS-403 K. Orito,
A New Variable Transformation Technique for the Nonlinear Drift Vortex; Feb. 1996

NIFS-404 T. Oike, K. Kitachi, S. Ohdachi, K. Toi, S. Sakakibara, S. Morita, T. Morisaki, H. Suzuki, S. Okamura, K. Matsuoka and CHS group; *Measurement of Magnetic Field Fluctuations near Plasma Edge with Movable Magnetic Probe Array in the CHS Heliotron/Torsatron*; Mar. 1996

NIFS-405 S.K. Guharay, K. Tsumori, M. Hamabe, Y. Takeiri, O. Kaneko, T. Kuroda,
Simple Emittance Measurement of H- Beams from a Large Plasma Source; Mar. 1996

NIFS-406 M. Tanaka and D. Biskamp,
Symmetry-Breaking due to Parallel Electron Motion and Resultant Scaling in Collisionless Magnetic Reconnection; Mar. 1996

NIFS-407 K. Kitachi, T. Oike, S. Ohdachi, K. Toi, R. Akiyama, A. Ejiri, Y. Hamada, H.Kuramoto, K. Narihara, T. Seki and JIPP T-IIU Group,
Measurement of Magnetic Field Fluctuations within Last Closed Flux Surface with Movable Magnetic Probe Array in the JIPP T-IIU Tokamak; Mar. 1996

NIFS-408 K. Hirose, S. Saito and Yoshi.H. Ichikawa
Structure of Period-2 Step-1 Accelerator Island in Area Preserving Maps; Mar. 1996

NIFS-409 G.Y.Yu, M. Okamoto, H. Sanuki, T. Amano,
Effect of Plasma Inertia on Vertical Displacement Instability in Tokamaks; Mar. 1996

NIFS-410 T. Yamagishi,

Solution of Initial Value Problem of Gyro-Kinetic Equation; Mar. 1996

NIFS-411 K. Ida and N. Nakajima,
Comparison of Parallel Viscosity with Neoclassical Theory; Apr. 1996

NIFS-412 T. Ohkawa and H. Ohkawa,
Cuspher, A Combined Confinement System; Apr. 1996

NIFS-413 Y. Nomura, Y.H. Ichikawa and A.T. Filippov,
Stochasticity in the Josephson Map; Apr. 1996

NIFS-414 J. Uramoto,
Production Mechanism of Negative Pionlike Particles in H_2 Gas Discharge Plasma; Apr. 1996

NIFS-415 A. Fujisawa, H. Iguchi, S. Lee, T.P. Crowley, Y. Hamada, S. Hidekuma, M. Kojima,
Active Trajectory Control for a Heavy Ion Beam Probe on the Compact Helical System; May 1996

NIFS-416 M. Iwase, K. Ohkubo, S. Kubo and H. Idei
Band Rejection Filter for Measurement of Electron Cyclotron Emission during Electron Cyclotron Heating; May 1996

NIFS-417 T. Yabe, H. Daido,T. Aoki, E. Matsunaga and K. Arisawa,
Anomalous Crater Formation in Pulsed-Laser-Illuminated Aluminum Slab and Debris Distribution; May 1996

NIFS-418 J. Uramoto,
Extraction of K^- Mesonlike Particles from a D_2 Gas Discharge Plasma in Magnetic Field; May 1996

NIFS-419 J. Xu, K. Toi, H. Kuramoto, A. Nishizawa, J. Fujita, A. Ejiri, K. Narihara, T. Seki, H. Sakakita, K. Kawahata, K. Ida, K. Adachi, R. Akiyama, Y. Hamada, S. Hirokura, Y. Kawasumi, M. Kojima, I. Nomura, S. Ohdachi, K.N. Sato
Measurement of Internal Magnetic Field with Motional Stark Polarimetry in Current Ramp-Up Experiments of JIPP T-IIU; June 1996

NIFS-420 Y.N. Nejoh,
Arbitrary Amplitude Ion-acoustic Waves in a Relativistic Electron-beam Plasma System; July 1996

NIFS-421 K. Kondo, K. Ida, C. Christou, V.Yu.Sergeev, K.V.Khlopenkov, S.Sudo, F. Sano, H. Zushi, T. Mizuuchi, S. Besshou, H. Okada, K. Nagasaki, K. Sakamoto, Y. Kurimoto, H. Funaba, T. Hamada, T. Kinoshita, S. Kado, Y. Kanda, T. Okamoto, M. Wakatani and T. Obiki,
Behavior of Pellet Injected Li Ions into Heliotron E Plasmas; July 1996

NIFS-422 Y. Kondoh, M. Yamaguchi and K. Yokozuka,
Simulations of Toroidal Current Drive without External Magnetic Helicity Injection; July 1996

NIFS-423 Joong-San Koog,
Development of an Imaging VUV Monochromator in Normal Incidence Region; July 1996

NIFS-424 K. Orito,
A New Technique Based on the Transformation of Variables for Nonlinear Drift and Rossby Vortices; July 1996

NIFS-425 A. Fujisawa, H. Iguchi, S. Lee, T.P. Crowley, Y. Hamada, H. Sanuki, K. Itoh, S. Kubo, H. Idei, T. Minami, K. Tanaka, K. Ida, S. Nishimura, S. Hidekuma, M. Kojima, C. Takahashi, S. Okamura and K. Matsuoka,
Direct Observation of Potential Profiles with a 200keV Heavy Ion Beam Probe and Evaluation of Loss Cone Structure in Toroidal Helical Plasmas on the Compact Helical System; July 1996

NIFS-426 H. Kitauchi, K. Araki and S. Kida,
Flow Structure of Thermal Convection in a Rotating Spherical Shell; July 1996

NIFS-427 S. Kida and S. Goto,
Lagrangian Direct-interaction Approximation for Homogeneous Isotropic Turbulence; July 1996

NIFS-428 V.Yu. Sergeev, K.V. Khlopenkov, B.V. Kuteev, S. Sudo, K. Kondo, F. Sano, H. Zushi, H. Okada, S. Besshou, T. Mizuuchi, K. Nagasaki, Y. Kurimoto and T. Obiki,
Recent Experiments on Li Pellet Injection into Heliotron E; Aug. 1996

NIFS-429 N. Noda, V. Philipps and R. Neu,
A Review of Recent Experiments on W and High Z Materials as Plasma-Facing Components in Magnetic Fusion Devices; Aug. 1996

NIFS-430 R.L. Tobler, A. Nishimura and J. Yamamoto,
Design-Relevant Mechanical Properties of 316-Type Stainless Steels for Superconducting Magnets; Aug. 1996

NIFS-431 K. Tsuzuki, M. Natsir, N. Inoue, A. Sagara, N. Noda, O. Motojima, T. Mochizuki, T. Hino and T. Yamashina,
Hydrogen Absorption Behavior into Boron Films by Glow Discharges in Hydrogen and Helium; Aug. 1996

NIFS-432 T.-H. Watanabe, T. Sato and T. Hayashi,
Magnetohydrodynamic Simulation on Co- and Counter-helicity Merging of Spheromaks and Driven Magnetic Reconnection; Aug. 1996

NIFS-433 R. Horiuchi and T. Sato,
Particle Simulation Study of Collisionless Driven Reconnection in a Sheared Magnetic Field; Aug. 1996

NIFS-434 Y. Suzuki, K. Kusano and K. Nishikawa,
Three-Dimensional Simulation Study of the Magnetohydrodynamic Relaxation Process in the Solar Corona. II.; Aug. 1996

NIFS-435 H. Sugama and W. Horton,
Transport Processes and Entropy Production in Toroidally Rotating Plasmas with Electrostatic Turbulence; Aug. 1996

NIFS-436 T. Kato, E. Rachlew-Källne, P. Hörling and K.-D Zastrow,
Observations and Modelling of Line Intensity Ratios of OV Multiplet Lines for 2s3s 3S1 - 2s3p 3Pj; Aug. 1996

NIFS-437 T. Morisaki, A. Komori, R. Akiyama, H. Idei, H. Iguchi, N. Inoue, Y. Kawai, S. Kubo, S. Masuzaki, K. Matsuoka, T. Minami, S. Morita, N. Noda, N. Ohyabu, S. Okamura, M. Osakabe, H. Suzuki, K. Tanaka, C. Takahashi, H. Yamada, I. Yamada and O. Motojima.
Experimental Study of Edge Plasma Structure in Various Discharges on Compact Helical System; Aug. 1996

NIFS-438 A. Komori, N. Ohyabu, S. Masuzaki, T. Morisaki, H. Suzuki, C. Takahashi, S. Sakakibara, K. Watanabe, T. Watanabe, T. Minami, S. Morita, K. Tanaka, S. Ohdachi, S. Kubo, N. Inoue, H. Yamada, K. Nishimura, S. Okamura, K. Matsuoka, O. Motojima, M. Fujiwara, A. Iiyoshi, C. C. Klepper, J.F. Lyon, A.C. England, D.E. Greenwood, D.K. Lee, D.R. Overbey, J.A. Rome, D.E. Schechter and C.T. Wilson,
Edge Plasma Control by a Local Island Divertor in the Compact Helical System; Sep. 1996 (IAEA-CN-64/C1-2)

NIFS-439 K. Ida, K. Kondo, K. Nagaski T. Hamada, H. Zushi, S. Hidekuma, F. Sano, T. Mizuuchi, H. Okada, S. Besshou, H. Funaba, Y. Kurimoto, K. Watanabe and T. Obiki,
Dynamics of Ion Temperature in Heliotron-E; Sep. 1996 (IAEA-CN-64/CP-5)

NIFS-440 S. Morita, H. Idei, H. Iguchi, S. Kubo, K. Matsuoka, T. Minami, S. Okamura, T. Ozaki, K. Tanaka, K. Toi, R. Akiyama, A. Ejiri, A. Fujisawa, M. Fujiwara, M. Goto, K. Ida, N. Inoue, A. Komori, R. Kumazawa, S. Masuzaki, T. Morisaki, S. Muto, K. Narihara, K. Nishimura, I. Nomura, S. Ohdachi, M.. Osakabe, A. Sagara, Y. Shirai, H. Suzuki, C. Takahashi, K. Tsumori, T. Watari, H. Yamada and I. Yamada,
A Study on Density Profile and Density Limit of NBI Plasmas in CHS; Sep. 1996 (IAEA-CN-64/CP-3)